

# Moonlighting glyceraldehyde-3-phosphate dehydrogenase of *Lactobacillus gasseri* inhibits keratinocyte apoptosis and skin inflammation in experimental atopic dermatitis

Pei-Chi Chen,<sup>1,2,3</sup> Miao-Hsi Hsieh,<sup>1</sup> Wei-Leng Chen,<sup>2</sup> Yu-Pu Hsia,<sup>2</sup> Wen-Shuo Kuo,<sup>1,4</sup> Lawrence Shih-Hsin Wu,<sup>1,5</sup> Shulhn-Der Wang,<sup>1,6</sup> Xiao-Yu Liu,<sup>7</sup> Jiu-Yao Wang,<sup>1,8</sup> Hui-Fang Kao<sup>3</sup>

## Abstract

**Background:** Atopic dermatitis (AD) is a chronic inflammatory skin disorder affecting up to 20% of children in developed countries. Although probiotics have shown promise as adjuvant treatments for AD, their mechanisms are not well understood.

**Objective:** Building upon our previous studies, we investigated whether *Lactobacillus gasseri* and its moonlighting glyceraldehyde 3-phosphate dehydrogenase (GAPDH), namely LGp40, could be beneficial in AD management.

**Methods:** In AD mouse models (SKH and C57BL/6J mice) with ovalbumin (OVA) and *Dermatophagoides pteronyssinus* (Der p) allergens, aligning with the “outside-in” and “inside-out” hypotheses, we administered *L. gasseri* orally and LGp40 intraperitoneally to investigate their protective effects. The evaluation involved measuring physiological, pathological, and immune function parameters. To delve deeper into the detailed mechanism of LGp40 protection in AD, additional assays were conducted using human skin keratinocytes (HaCaT) and monocytes (THP1) cell lines.

**Results:** *L. gasseri* and LGp40 enhanced skin barrier function and increased skin moisture retention. They also led to reduced infiltration of Langerhans cells in the dermis and mitigated skewed Th2 and Th17 immune responses. Moreover, LGp40 inhibited allergen-induced keratinocyte apoptosis through the blockade of the caspase-3 cascade and reduced the NLR family pyrin domain containing 3 (NLRP3) inflammasome in macrophages. These inhibitions were achieved through the activation of the peroxisome proliferator-activated receptor gamma (PPAR $\gamma$ ) pathway.

**Conclusion:** The results of this study provide a novel insight into the mechanism of action of probiotics in the prevention and treatment for allergic disorders through the moonlighting GAPDH protein.

**Key words:** atopic dermatitis, Lactobacilli, glyceraldehyde-3-phosphate dehydrogenase (GAPDH), peroxisome proliferator-activated receptor gamma (PPAR $\gamma$ ), apoptosis

## Citation:

Chen, P. C., Hsieh, M. H., Chen, W. L., Hsia, Y. P., Kuo, W. S., Wu, L. S. H., Wang, S. D., Liu, X. Y., Wang, J. Y., Kao, H. F. (0000). Moonlighting glyceraldehyde-3-phosphate dehydrogenase of *Lactobacillus gasseri* inhibits keratinocyte apoptosis and skin inflammation in experimental atopic dermatitis. *Asian Pac J Allergy Immunol*, 00(0), 000-000. <https://doi.org/10.12932/ap-211123-1733>

## Affiliations:

- <sup>1</sup> Center for Allergy, Immunology, and Microbiome (A.I.M.), China Medical University Hospital, Taichung, Taiwan
- <sup>2</sup> Department of Microbiology & Immunology, College of Medicine, National Cheng Kung University, Tainan, Taiwan
- <sup>3</sup> Department of Nursing, National Tainan Junior College of Nursing, Tainan, Taiwan
- <sup>4</sup> School of Chemistry and Materials Science, Nanjing University of Information Science and Technology, Nanjing, China
- <sup>5</sup> Graduate Institute of Biomedical Sciences, China Medical University, Taichung, Taiwan
- <sup>6</sup> School of post-baccalaureate Chinese Medicine, China Medical University, Taichung, Taiwan
- <sup>7</sup> Research Center of Allergy & Immunology, Shenzhen University School of Medicine, Shenzhen, China
- <sup>8</sup> Department of Allergy, Immunology, and Rheumatology (AIR), China Medical University Children's Hospital, Taichung, Taiwan

**Corresponding author:**

1. Hui-Fang Kao  
Department of Nursing, National Tainan Junior College of Nursing,  
No. 78, Section 2, Minzu Rd, West Central District, 700,  
Tainan, Taiwan  
E-mail: kaohf@ntin.edu.tw
2. Jiu-Yao Wang  
Center of Allergy, Immunology, and Microbiome (A.I.M.),  
China Medical University Hospital,  
No. 2, Yuh-Der Road, Taichung city, 404, Taiwan  
E-mail: wangjy@mail.cmu.edu.tw

## Introduction

Atopic dermatitis (AD) is a common allergic skin disorder that is characterized by chronic relapsing skin inflammation, disruption of the epidermal barrier function, and keratinocyte apoptosis.<sup>1</sup> The complex etiology of AD includes genetic risks, environmental factors, immunoglobulin E (IgE)-mediated hypersensitivity, different T cell subtypes-driven inflammation, and skin microbiome diversity.<sup>1</sup> Disruption of the skin barrier permits unrestricted allergens entry into the skin that triggers the release of alarmin-like thymic stromal lymphopoietin (TSLP), IL-25, and IL-33 from keratinocytes, which induced group 2 innate lymphoid cells (ILC2) to drives type 2 inflammatory responses.<sup>1</sup> Upon allergen exposure, Langerhans cells – which constitute the epithelial-resident dendritic cell – present antigens to trigger type 2 helper T cells (Th2) development.<sup>1</sup> The sked Th2 immunity then promotes IgE and eosinophil mediated responses. Furthermore, the infiltration of interleukin (IL)-17<sup>+</sup> cells into AD skin lesions contributes to the pathology and provides a defense system against bacterial invasion.<sup>2</sup>

The pathogenesis of AD is mainly propounded in two hypotheses: the “outside-in” hypothesis implies that inherent damage resulting in the disruption of the epidermal barrier facilitates the entry of allergens and results in immunologic imbalance; the “inside-out” hypothesis suggests that the immunological cascade triggers skin barrier impairment, leading to the AD phenotype.<sup>3</sup> Moreover, an abnormal increase in keratinocyte apoptosis was found to increased AD exacerbations.<sup>4</sup> Keratinocyte apoptosis is induced by skin-infiltrating T-cell-mediated Fas/Fas ligand molecular interactions and subsequent caspase activation and increased expression of cleaved caspase-3 in skin lesions in acute AD.<sup>4,5</sup> Therefore, prevention of keratinocyte apoptosis is a potential therapeutic strategy for alleviating atopic skin inflammation.

Early-life oral supplementation with *Lactobacillus* or/and *Bifidobacterium* has a long-term preventive effect against AD by impeding the development and onset of allergic symptoms.<sup>6</sup> Previously, our double-blind randomized placebo-controlled trail in Taiwan revealed that a probiotic mixture of *Lactobacillus* species attenuated clinical symptoms in moderate-to-severe AD in children.<sup>7</sup> Moreover, oral intake of *L. gasseri* inhibits airway inflammation in allergic asthma through the activation of the peroxisome proliferator-activated receptor  $\gamma$  (PPAR $\gamma$ ) pathway in dendritic cells and inhibited Th2 and Th17 immune response.<sup>8,9</sup> Furthermore, the glyceraldehyde-3-phosphate dehydrogenase (GAPDH) protein has been identified

and purified as the anti-allergic inflammation and PPAR $\gamma$  activation component in *L. gasseri* by our group.<sup>10</sup> GAPDH is a moonlighting protein that has multiple functions beyond its glycolytic enzymatic activity. The multifaceted non-enzymatic attributes of bacterial GAPDH are contingent upon its subcellular localization. Intracellularly, it contributes to gene expression and facilitates DNA repair mechanisms. On the bacterial cell surface, it engages with host proteins to enhance bacterial invasiveness. Extracellularly, it may exert influence on the host’s immune response.<sup>11</sup> These findings confirm that probiotic, their metabolites, and cellular components have important immunoregulatory roles in the prevention and treatment of allergic disease.

The present study was conducted to evaluate the preventive and therapeutic effects of *L. gasseri* and its moonlighting GAPDH in experimental atopic dermatitis induced by ovalbumin (OVA) and *Dermatophagoides pteronyssinus* (Der p) allergens via “outside-in” or “inside-out” route.

## Methods

### Allergen, *L. gasseri*, and LGp40

The Der p (Allergon, Sweden) or OVA (A5503, albumin from chicken egg white, Sigma-Aldrich, USA) allergen was dissolved in sterile phosphate-buffered saline (PBS) and filtered separately through a 0.22- $\mu$ m filter. *L. gasseri* (BCRC14619) was cultured in MRS Broth (110661, Merk Millipore, USA) at 37°C. Recombinant His-tagged LGp40 was purified by loading onto an Ni-NTA and Q column (GE Healthcare, USA) as described previously.<sup>10</sup>

### Animal experimental models and protocols

The 6- to 8-week-old mice used in this study included SKH1 (hairless) mice, and C57BL/6J mice, which were purchased from National Applied Research Laboratories, Taiwan. Mice were housed in sterile cages with an air-filtration device in the Laboratory Animal Center of the College of Medicine, National Cheng Kung University, Tainan, Taiwan. All animal experiments were performed according to protocols approved by the Institutional Animal Care and Use Committee of National Cheng Kung University, Tainan, Taiwan (IACUC No. 101221).

**Protocol 1:** To establish an “outside-in” model of AD, the SKH1 and C57BL/6J mice were divided into four groups that were to be subjected to epicutaneous sensitization with different agents. After anesthetization, the dorsal skin of the C57BL/6J mice was shaved to expose the skin. To the dorsal skin of C57BL/6J and SKH1 mice, we then applied a 1×1cm square of sterile gauze saturated with a 100  $\mu$ l PBS solution containing 100  $\mu$ g OVA (OVA group), 50  $\mu$ g Der p extract (Der p group), or PBS (PBS group) for 7 consecutive days. Mice were sensitized three times, at 2-week intervals. To identify the protective effect of *L. gasseri*, OVA-induced AD SKH1 mice were intragastrically administered 200  $\mu$ l of PBS (PBS group), 200  $\mu$ l PBS of a solution containing 10<sup>7</sup> colony-forming unit (CFU) *L. gasseri*

( $10^7$  LG group), or 200  $\mu$ l PBS of a solution containing  $10^9$  CFU *L. gasseri* ( $10^9$  LG group) daily during the OVA-sensitization period. To determine the effect of LGp40, both OVA- and Der p-induced AD SKH1 mice were intraperitoneally injected with 200  $\mu$ l of PBS or 200  $\mu$ l PBS of a solution containing 25  $\mu$ g LGp40 on days 1, 21, and 42.

**Protocol 2:** To establish an “inside-out” model of AD at C57BL/6J mice, the subcutaneous challenge (SC group) and epicutaneous challenge (EC group) mice were intraperitoneally sensitized with a 200  $\mu$ l mixture of 100  $\mu$ g Der p and 1 mg aluminum hydroxide (Al(OH)<sub>3</sub>, Thermo Fisher, USA) on days 0 and 7. For SC group of C57BL/6J mice, furs of their dorsal skins were removed for further subcutaneous allergen injections with 100  $\mu$ g/100  $\mu$ l Der p every 3 days for totally three times, whereas the EC mice were epicutaneously challenged through skin coverage by a 1  $\times$  1 cm square of sterile gauze saturated with a 100  $\mu$ l PBS solution containing 100  $\mu$ g Der p for 3 consecutive days three times. Control (Ctrl group) mice were sensitized with 1 mg Al(OH)<sub>3</sub> and challenged with PBS. To determine the effect of LGp40, Der p-induced AD C57BL/6J mice were intraperitoneally injected with 200  $\mu$ l of PBS (PBS group), 200  $\mu$ l PBS of a solution containing 25  $\mu$ g LGp40 (LGp40 group), or 200  $\mu$ l PBS of a solution containing 10  $\mu$ g dexamethasone (Dex, 265005, Sigma-Aldrich; Steroid group) on days 1, 21, and 42. At the end of each model, the physiological function of the dorsal skin of the mice was measured before the mice were sacrificed, and the lesion skin, blood, and spleen were harvested for further analysis.

#### **Transepidermal water loss (TEWL) measurement**

TEWL measurements of the dorsal skin lesions were performed using Tewameter TM210 (Courage and Khazaka Electronic GmbH, Germany). The temperature and relative humidity of the measurement rooms remained consistent throughout the procedure. Measurements were recorded as g/m<sup>2</sup>/h after the rate of TEWL had stabilized. Mice were anesthetized to facilitate the measurements. The Tewameter probe was gently placed against the skin surface at the site where the patch containing the allergen had been applied, and the readings were recorded for 1 min. An average of the three readings was used as the TEWL for each mouse.

#### **Total and allergen-specific IgE measurement**

Total IgE levels in sera were assayed using enzyme-linked immunosorbent assay (ELISA; E90-115, Bethyl Laboratories, USA). For allergen-specific IgE quantification, the plates were first coated with 10  $\mu$ g Der p or 10  $\mu$ g OVA at 4°C for 18 hours. After blocking, diluted sera (1:50 dilution) were added and the plates were incubated overnight at 4°C with horseradish peroxidase (HRP)-conjugated secondary antibodies (E90-115, Bethyl Laboratories); then, the optical density was determined at 450 nm.

#### **Skin histology and immunohistochemistry (IHC)**

The dorsal skin tissue was removed, fixed in 10% formalin (SI-F8775, Sigma-Aldrich), and embedded in paraffin. Sections (4- $\mu$ m thick) were stained with hematoxylin and eosin kit (H&E; HAE-1, ScyTek Laboratories, USA) or immunostaining. For IHC, the samples were incubated with anti-TSLP (4025, ProSci, USA), anti-Langerin/CD207 (DDX0362, Dendritics, France), anti-RAR-related orphan receptor gamma t (ROR $\gamma$ t; bs-6217R, Bioss, USA), anti-IL-17 (Ab79056, Abcam, UK), and anti-cytokeratin 18-fragment M30 (MA5-12104, ThermoFisher) antibodies. The immunoreactivity of Langerin/CD207 was visualized using the AEC immunophosphatase methodology (001122, ThermoFisher) whereas the immunoreactivity of the other antibodies was visualized using the DAB immunoperoxidase methodology with the Novolink™ Polymer Detection Systems kit (RE7140-K, Leica, UK).

#### **Cytokine measurement of splenocyte culture supernatant**

Spleens were isolated and homogenized into single-cell suspensions through a 70- $\mu$ m cell strainer. Cells were seeded at a density of  $1 \times 10^6$  cells/mL in RPMI-1640 containing 10% FBS (ThermoFisher) and were stimulated with 8  $\mu$ g phytohemagglutinin (PHA; L4144, Sigma-Aldrich) for 48 hours. Cultured supernatants were collected and the levels of IFN- $\gamma$ , IL-17, and IL-10 were determined using commercial ELISA kits (DY485, DY421, DY417, R&D Systems, USA).

#### **Apoptosis induction in HaCaT cells.**

The HaCaT cell line was cultured at 37°C in DMEM supplemented with 10% fetal bovine serum (FBS, ThermoFisher). HaCaT cells were plated in 6-well plates at a density of  $1 \times 10^6$  cells/well. The culture medium was replaced by DMEM-2% FBS for apoptosis induction. Cells were incubated with 10  $\mu$ M GW9662 (M6191, Sigma-Aldrich), 10  $\mu$ M rosiglitazone (RO; R2408, Sigma-Aldrich), LGp40 (1 or 10  $\mu$ g/mL), and LGp40 (1 or 10  $\mu$ g/mL) + 10  $\mu$ M GW9662 for 6 hours. Thereafter, cells were further stimulated with 12.5  $\mu$ g/mL Der p for 24 hours. Cultured cells were then collected for flow cytometry and Western blot analysis.

#### **NLR family pyrin domain containing the 3 (NLRP3) inflammasome activation in THP1 cells**

The THP1 cell line was cultured at 37°C in RPMI-1640 supplemented with 10% FBS (ThermoFisher). THP1 cells were plated in 6-well plates at a density of  $1 \times 10^6$  cells/well. Cells were first differentiated using 100 ng/mL phorbol-12-myristate-13-acetate (PMA; SI-P1585, Sigma-Aldrich) for 72 hours, and then rested for 24 hours. The differentiated THP1 cells were then incubated with LGp40 (5, 10, 20  $\mu$ g/mL) for 4, 6, or 12 hours or 10  $\mu$ g/mL LGp40 + GW9662 (1, 5, or 10  $\mu$ M) for 6 hours.

Next, NLRP3 inflammasome activation of the cells was established using 5 µg/mL lipopolysaccharide (LPS; L9764, Sigma-Aldrich) for 18 hours, followed by 5 mM adenosine triphosphate (ATP; tlr-atpl, InvivoGen, USA) 1-hour stimulation. Cultured cells were then collected for Western blot analysis.

### Flow cytometric detection of apoptosis

Primary keratinocytes from the C57BL/6J mouse dorsal skin (animal experimental model protocol 2) and HaCaT cells were prepared at a density of  $1 \times 10^6$ /mL for flow cytometric detection of apoptosis using FITC Annexin V Apoptosis Detection Kit with 7-AAD (640922, BioLegend, USA). Cells were gated at 10,000 events and analyzed using FACS Calibur™ (BD Bioscience, USA).

### Western blot analysis

Whole-cell lysates were prepared with the Radio-Immuno-precipitation Assay (RIPA) buffer (Sigma-Aldrich) and then boiled in sample buffer at 99°C for 15 minutes. Samples containing 30 µg of total protein were electrophoresed on 12% SDS-PAGE and transferred onto PVDF membranes (Merck Millipore, USA) that were blocked for 1 hour with 10% non-fat milk in TBST, and incubated overnight with the following antibodies: pro-caspase-3 (ARG20001, arigo biolaboratories, Taiwan), cleaved caspase-3 (ARG57512, arigo biolaboratories), PPARγ (101700, Cayman Chemical, USA), NLRP3 (AG-20B-0014-C100, adipogen life sciences, USA), and β-actin (GTX109639, GeneTex, USA). After incubated with HRP-conjugated secondary antibodies (GTX221667-01 and

GTX221666-01, GeneTex), membranes were treated with the Western lightning chemiluminescence reagent (PerkinElmer, USA) and visualized using an X-ray film. The density of the detected proteins was calculated in relation to the density of β-actin and the results were presented as a proportion.

### Statistical analysis

All data were presented as mean ± SEM and analyzed with the Student's *t*-test by using GraphPad Prism software (San Diego, USA).

## Results

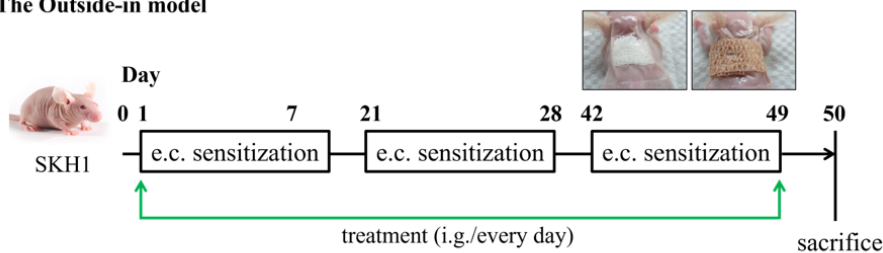
### The “outside-in” and “inside-out” mouse models of AD

In this study, the protection effect of *L. gasseri* and its moonlighting recombinant GAPDH (LGp40) were investigated in the “outside-in” and “inside-out” mouse models of AD. The clinical characteristics of these two models of AD were detailed in **Supplemental File** and **Supplemental Figure 1-4**.

### *L. gasseri* attenuated cutaneous inflammation in OVA-induced SKH1 AD-like mice

The OVA epicutaneously sensitized SKH1 AD-like mice were intra-gastrically administered different dosages (low,  $10^7$  CFU or high,  $10^9$  CFU) of *L. gasseri* or PBS control for 7 weeks (**Figure 1A**).  $10^7$  CFU of *L. gasseri* treatment reduced total IgE and significantly lowered OVA-specific IgE levels as compared to PBS controls (**Figure 1B**). The characteristic atopic skin appearance improved after *L. gasseri* treatment and became unwrinkled and hydrated in the  $10^7$  and  $10^9$  CFU LG groups (**Figure 1C**). Histological analysis demonstrated a notable reduction in epidermal and

### A The Outside-in model



Group	e.c. sensitization	treatment (i.g./every day)
AD	100µg OVA in 100µl PBS	—
PBS	100µg OVA in 100µl PBS	PBS
$10^7$ LG	100µg OVA in 100µl PBS	$10^7$ CFU <i>L.gasseri</i>
$10^9$ LG	100µg OVA in 100µl PBS	$10^9$ CFU <i>L.gasseri</i>

**Figure 1. *L. gasseri* supplementation improved pathophysiological function and allergic inflammation in OVA-induced AD mice.** (A) Oral administration of *L. gasseri* in the OVA-induced AD SKH1 model based on the “outside-in” hypothesis. OVA-epicutaneously (e.c.) sensitized AD mice were intragastrically (i.g.) treated with either PBS and  $10^7$  or  $10^9$  CFU of *L. gasseri* orally (animal experimental model protocol 1). (B) Total IgE and OVA-specific IgE levels in sera were measured using ELISA. (C) Morphology of the skin lesion. (D) Lesional skin histology. (E) Measurement of epidermal and dermal thickness (\*\**p* < 0.01 of epidermis, †*p* < 0.05, ††*p* < 0.01 of dermis). (F) Infiltrated eosinophils in the cutaneous tissue were counted (††*p* < 0.01 of dermis). Skin sections were immunostained with (G) langerin/CD207 antibody, and (H) the positive cells (black arrows) in the cutaneous tissue were counted (†*p* < 0.05, ††*p* < 0.01 of dermis). Skin sections were immunostained with (I) TSLP and (J) IL-17 antibodies. (K) IFN-γ, IL-17, and IL-10 levels in the culture supernatant of splenocytes after PHA stimulation. The data represent the mean ± SEM (n = 4 mice), \**p* < 0.05, \*\**p* < 0.01, Student's *t*-test.



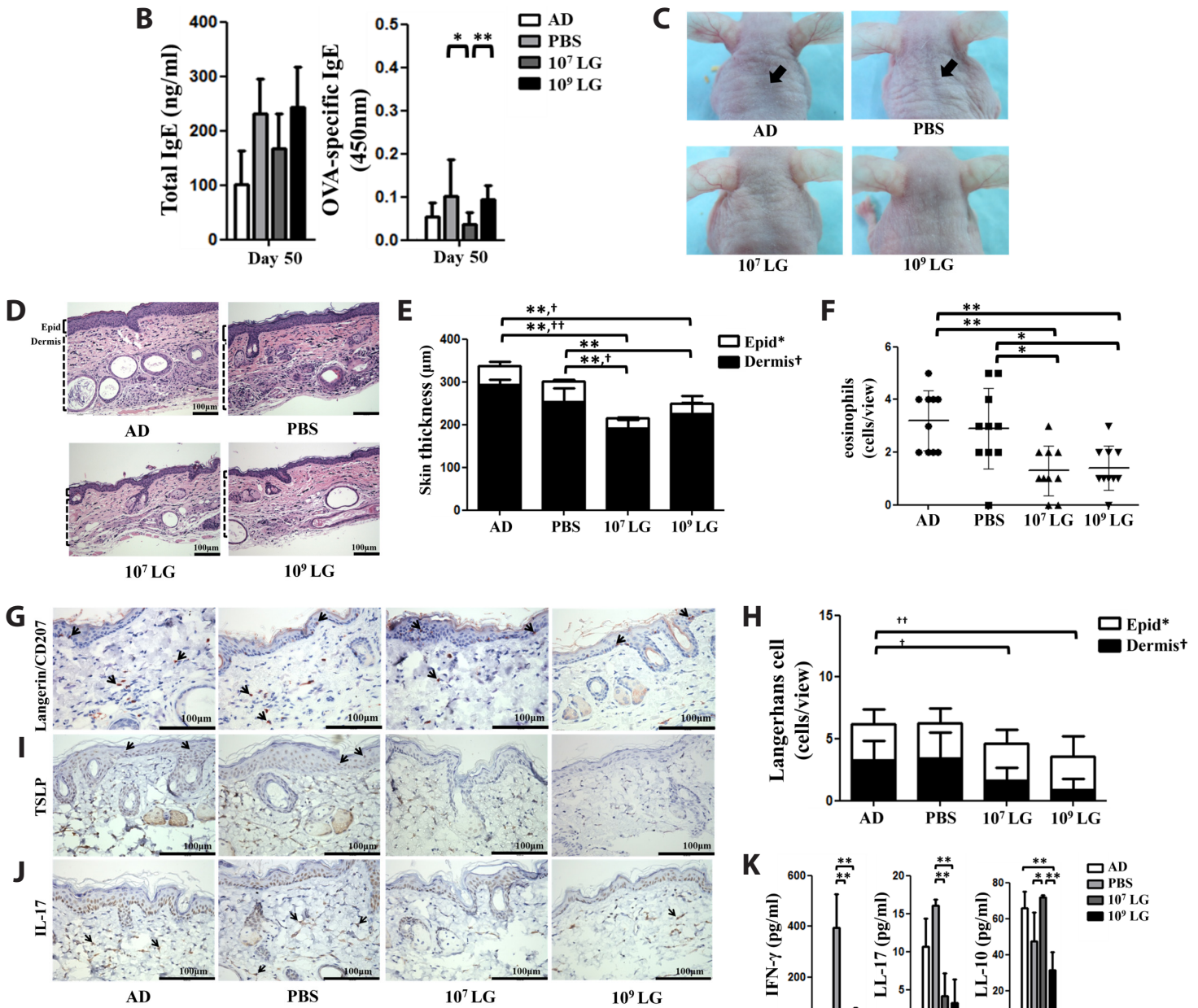
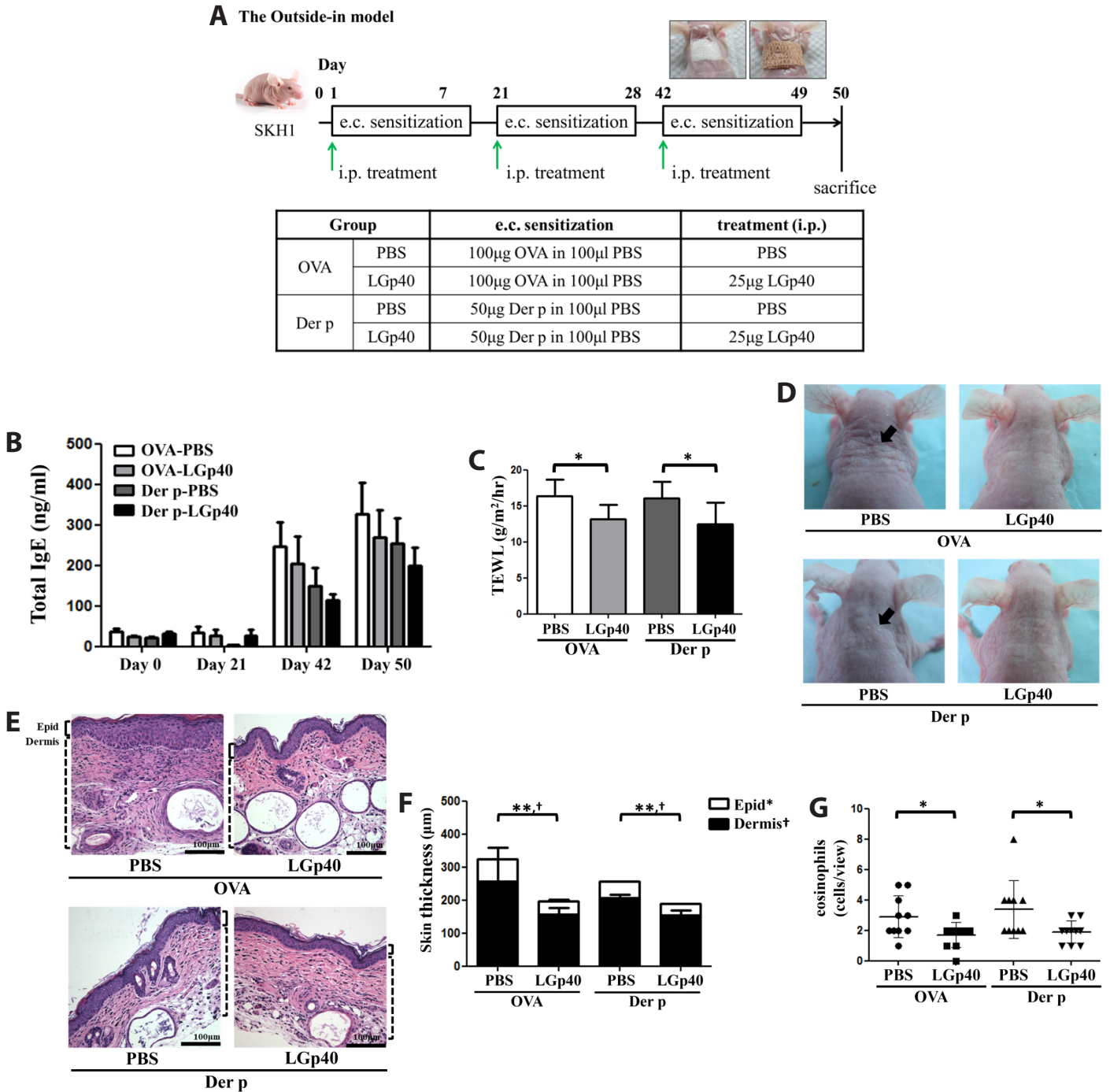


Figure 1. (Continued)

dermal thickness of both *L. gasseri*-treated groups compared to either the AD or PBS group (Figure 1D, E). The administration of *L. gasseri* in both low and high doses significantly inhibited OVA-induced cutaneous eosinophil and Langerhans cell infiltration of the dermis (Figure 1F-H). The expression of TSLP and IL-17 in the dorsal skin lesions were lower in 10<sup>7</sup> and 10<sup>9</sup> LG groups compared to those of the AD and PBS groups (Figure 1I, J). In response to *in vitro* stimulation with PHA, splenocytes from 10<sup>7</sup> and 10<sup>9</sup> LG mice secreted significantly lower amounts of IFN-γ and IL-17, as compared to the splenocytes from PBS mice. In contrast, the IL-10 level increased in 10<sup>7</sup> LG mice but decreased in 10<sup>9</sup> LG mice compared to the PBS mice (Figure 1K). Overall, oral treatment with *L. gasseri* improved OVA-induced atopic inflammation in the skin.

#### *LGp40* improved AD pathogenesis in the “outside-in” SKH1 AD-like mice

To explore the anti-allergic effect of the cellular component of *L. gasseri*, which was identified as GAPDH from *L. gasseri* that has a PPARγ activation effect in our previously report,<sup>10</sup> SKH1 mice were epicutaneously sensitized with either OVA or Der p to create the “outside-in” AD model as described earlier. Recombinant GAPDH of *L. gasseri* expressed from *E. coli*, LGp40 (25 µg), were intraperitoneally injected before each allergen epicutaneous-sensitization period (Figure 2A). The LGp40 decreased either OVA or Der p-induced total IgE production at days 42 and 50 after allergen sensitization and significantly reduced TEWL in comparison with the PBS-treated group (Figure 2B, C).



**Figure 2. Intraperitoneal administration of LGp40 repressed pathophysiological functions and allergic inflammation in the “outside-in” AD model.** (A) Intraperitoneal injection of LGp40 in the AD SKH1 model based on the “outside-in” hypothesis. Mice were epicutaneously (e.c.) sensitized with either OVA or Der p, and were intraperitoneally (i.p.) treated with either PBS or LGp40 (animal experimental model protocol 1). (B) Total IgE levels in sera were measured using ELISA. (C) TEWL values of skin were measured by Tewameter TM210. (D) Morphology of the lesional skin. (E) Lesional skin histology. (F) Measurement of the epidermal and dermal thickness (\*\* $p < 0.01$  of epidermis, † $p < 0.05$  of dermis). (G) Infiltrated eosinophils in the cutaneous tissue were counted († $p < 0.05$  of dermis). Skin sections were immunostained with (H) langerin/CD207 antibody, and (I) the positive cells (black arrows) in the cutaneous tissue were counted († $p < 0.05$  of dermis). Skin sections were immunostained with (J) TSLP, and (K) IL-17 antibodies. (L) IFN- $\gamma$  and (M) IL-17 production from the culture supernatant of splenocytes after PHA stimulation. The data represent the mean  $\pm$  SEM ( $n = 6$  mice), \* $p < 0.05$ , \*\* $p < 0.01$ , Student’s t-test.

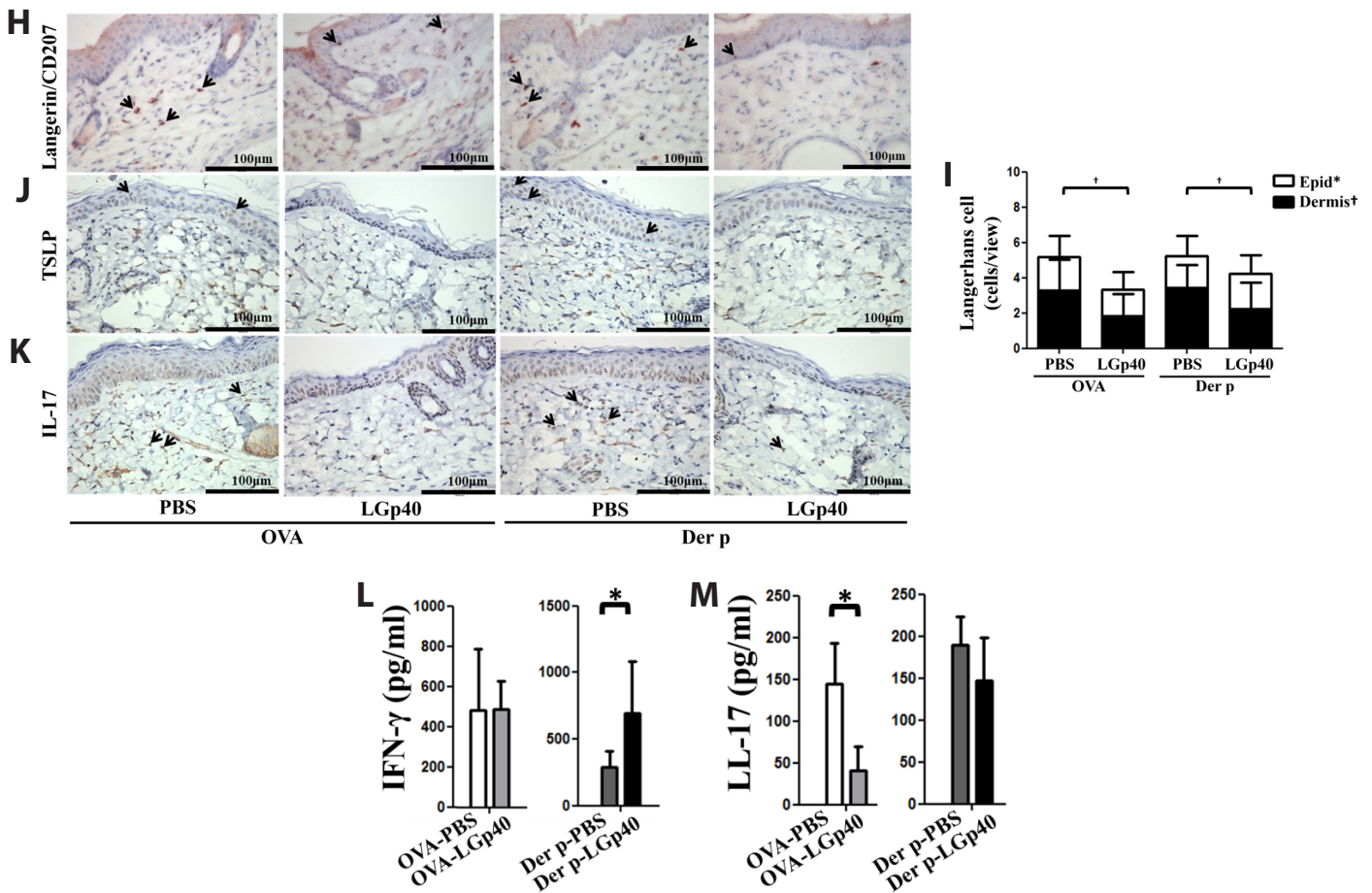


Figure 2. (Continued)

Smooth, moisturized skin was observed in the LGp40-treated mice, which also had normalized layers of epidermal and dermal thickness as compared to the untreated AD mice. (Figure 2D-F). The numbers of infiltrated eosinophils and Langerhans cells in the dermis decreased in the LGp40-treated groups (Figure 2G-I). Furthermore, the expression of TSLP and IL-17 in the skin lesions were inhibited by LGp40 (Figure 2J-K). Splenocytes from LGp40-treated Der p-induced AD-like mice produced significantly higher amounts of IFN- $\gamma$  in response to *in vitro* stimulation with PHA as compared to that in the PBS-treated mice (Figure 2L). Splenocytes from LGp40 treated mice had lower amounts of IL-17 as compared to PBS-treated mice. However, a significant difference was only found in the OVA-induced AD group (Figure 2M). These results showed that LGp40 improved atopic inflammation in a prevention manner in “outside-in” AD model.

#### LGp40 alleviated allergic skin inflammation in “inside-out” C57BL/6J AD-like mice

Either PBS, LGp40 (25  $\mu$ g), or Dex (1 mg/kg body weight) was intraperitoneal administration to C57BL/6J AD-like mice after each epicutaneous challenge (Figure 3A). Compared to naïve and Ctrl mice, the total IgE concentration significantly increased in the PBS-treated AD-like mice but decreased significantly after treatment with LGp40 or Dex as compared to non-treated AD mice (Figure 3B). The level of TEWL was significantly decreased after treatment with LGp40 or Dex as compared to the level in PBS-treated AD mice (Figure 3C). The typical wrinkled AD lesion along with prominent hair follicles, and inflamed, shiny skin became smooth and ruddy when the AD mice received either LGp40 or Dex. The hair even grew from the hair follicles in the LGp40-administered AD group (Figure 3D). After either LGp40 or steroid treatment, there was a significant decrease in the epidermal and dermal skin thickness, eosinophil and Langerhans cell infiltrations, and TSLP expression as compared to PBS-treated mice (Figure 3E-J). Taken together, the results showed that LGp40 alleviated the clinical symptoms of AD and decreased cutaneous inflammatory responses in AD-like mice, either in the “outside-in” or the “inside-out” models.



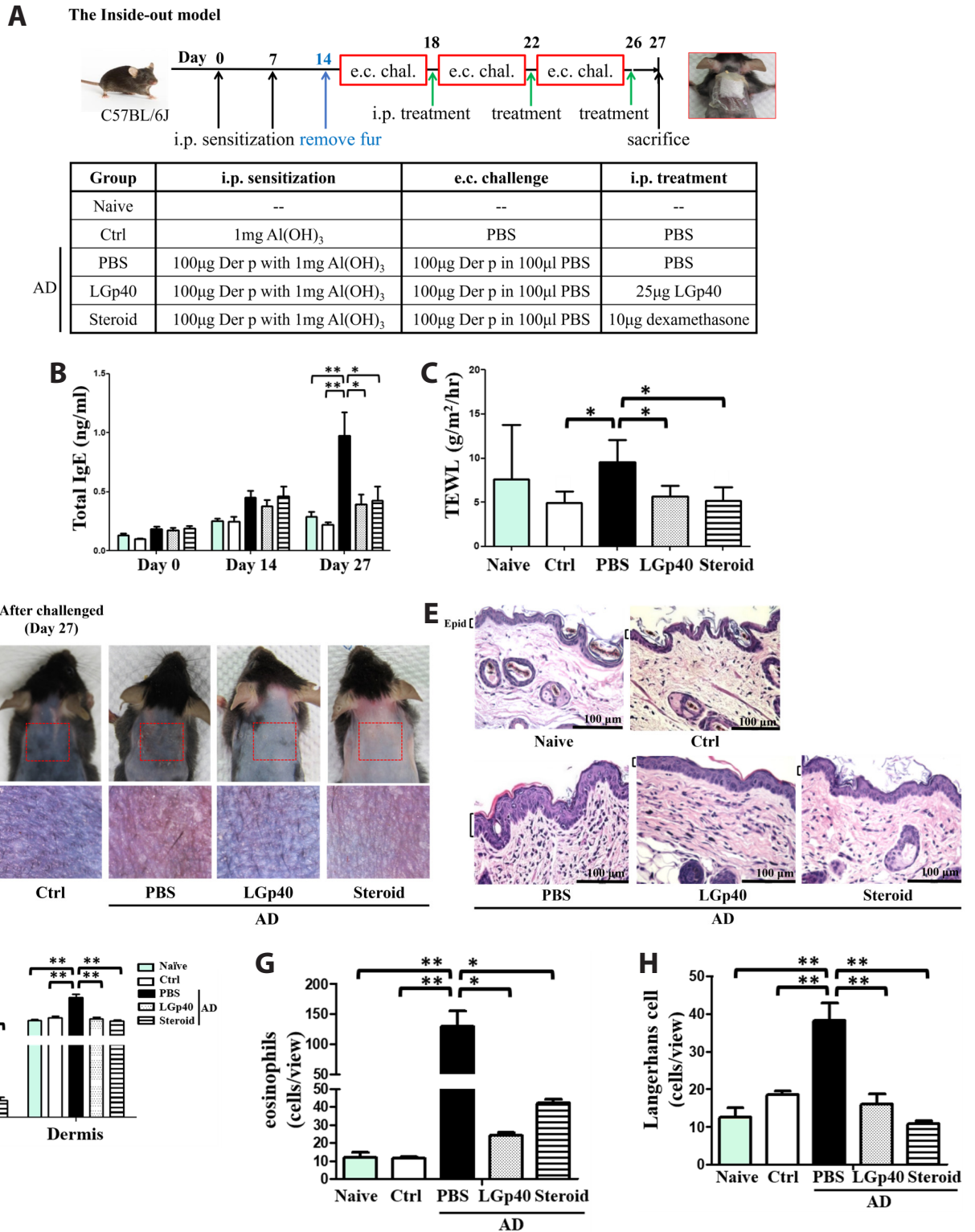


**Figure 3. Intraperitoneal administration of LGp40 alleviated pathophysiological functions and allergic inflammation in the “inside-out” AD model.** (A) LGp40 administration in the AD C57BL/6J model based on the “inside-out” hypothesis. Mice were divided into five groups. The naïve group was untreated. The Ctrl group was intraperitoneally (i.p.) sensitized and i.p. treated with PBS. The other groups were i.p. sensitized and epicutaneously (e.c.) challenge with Der p to induce AD, and received i.p. PBS, LGp40, or dexamethasone (Steroid group) based on the animal experimental model protocol 2. (B) Total IgE levels in sera were measured using ELISA. (C) TEWL values of skin were measured by Tewameter TM210. (D) Morphology of lesional skin. (E) Lesional skin histology. (F) Measurement of epidermal and dermal thickness. (G) Infiltrated eosinophils in the cutaneous tissue were counted. Skin sections were immunostained with (H) langerin/CD207 antibody, and (I) the positive cells (black arrows) in the cutaneous tissue were counted. Skin sections were immunostained with (J) TSLP antibodies and treated with DAB. The data represent the mean ± SEM (n ≥ 3 mice), \*p < 0.05, \*\*p < 0.01, Student’s t-test.



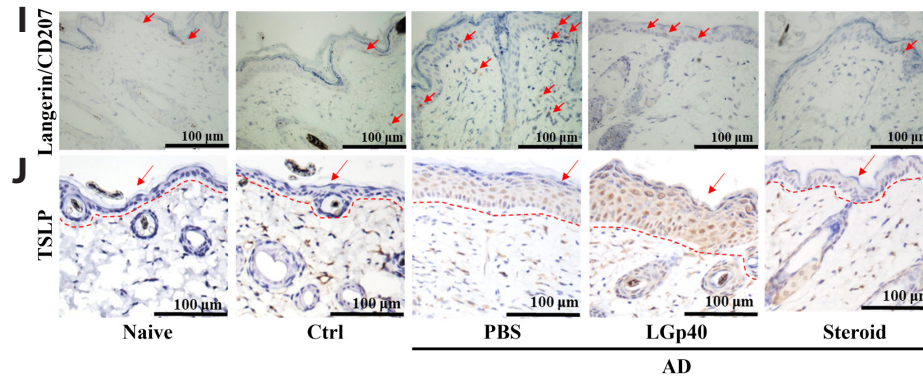
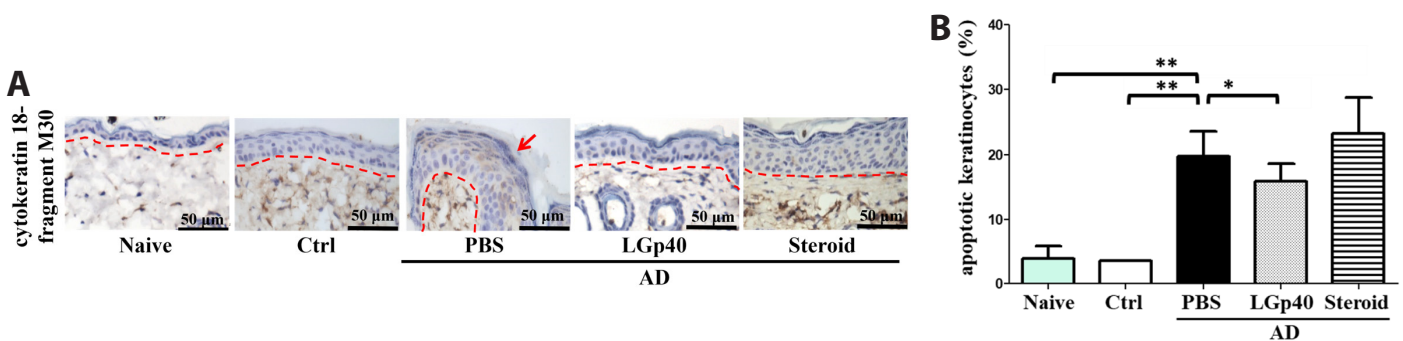


Figure 3. (Continued)

#### LGp40 inhibits keratinocyte apoptosis by upregulating PPAR $\gamma$ expression

The AD lesions of these mice were further analyzed to investigate the biological functions of LGp40 on the skin barrier. We found the increased expression of M30, a neo-epitope in cytokeratin 18 that becomes available during early caspase cleavage in apoptosis, in the epidermis of PBS-treated AD-like mice via IHC staining, as compared to naïve and ctrl mice. After treatment with LGp40 or Dex, the M30 expression in the lesion epidermis was significantly reduced (Figure 4A). Primary keratinocytes from skin lesion were harvested to measure apoptosis via flow cytometry. The percentage of apoptotic keratinocytes was significantly increased in PBS-treated AD-like mice, but significantly decreased in the LGp40-treated group although it did not in Dex-treated mice (Figure 4B). In skin lesions evaluated via Western blot analysis, expression of pro-caspase 3 and caspase-3 significantly increased in PBS treated AD-like mice,

Dex-treated groups (Figure 4C-E). The anti-apoptotic effect of LGp40 was assayed *in vitro* in Der p-induced apoptosis HaCaT cells. LGp40 (1  $\mu$ g/mL) pretreatment reduced the percentage of Der p-induced apoptotic cells and pro-caspase 3 and caspase-3 expressions, as compared to those of non-pretreatment condition (Figure 4F-G). The PPAR $\gamma$  activation effect of LGp40 also involved in its anti-apoptotic pathway. When GW9662, the PPAR $\gamma$  antagonist, was added with cell cultures, it blocked the anti-apoptotic effect of LGp40 on HaCaT cells. Pretreatment with a mixture of GW9662 and LGp40 increased the percentage of Der p-induced apoptotic cells as well as pro-caspase 3 and caspase-3 expressions as compared to LGp40-only pre-treatment HaCaT cells (Figure 4F, G). These results suggested that the inhibition of LGp40 in allergen-induced keratinocytes apoptosis may be mediated through the upregulation of the PPAR $\gamma$  pathway.



**Figure 4. LGp40 inhibited allergen-induced keratinocyte apoptosis in Der p-induced AD mice and it suppressed HaCaT cell apoptosis through upregulation of PPAR $\gamma$  expression.** (A) Skin sections were immunostained with cytokeratin 18 antibodies and treated with DAB. The region above the red-dotted line and arrows indicate cytokeratin 18 signals (brown) in the epidermis of lesional skin. (B) Apoptotic keratinocyte percentages in lesional skin suspension were determined using FACS. (C) Keratinocytes from lesional skin were analyzed by Western blotting with caspase 3 and  $\alpha$ -tubulin antibodies. Quantitative data of (D) pro-caspase 3 and (E) caspase 3. Protein expression levels were detected with densitometry and are depicted as proportional lines and bar graphs. The data represent the mean  $\pm$  SEM ( $n \geq 3$  mice), \* $p < 0.05$ , \*\* $p < 0.01$ , Student's *t*-test. HaCaT cells were incubated with rosiglitazone (RO, PPAR $\gamma$  agonist), GW9662 (PPAR $\gamma$  antagonist), LGp40, or LGp40 + GW9662 before Der p stimulation. (F) Apoptotic cell percentages were determined using FACS. (G) Whole-cell extracts were analyzed by Western blotting with caspase 3, PPAR $\gamma$ , and  $\beta$ -actin antibodies ( $n = 3$ ).

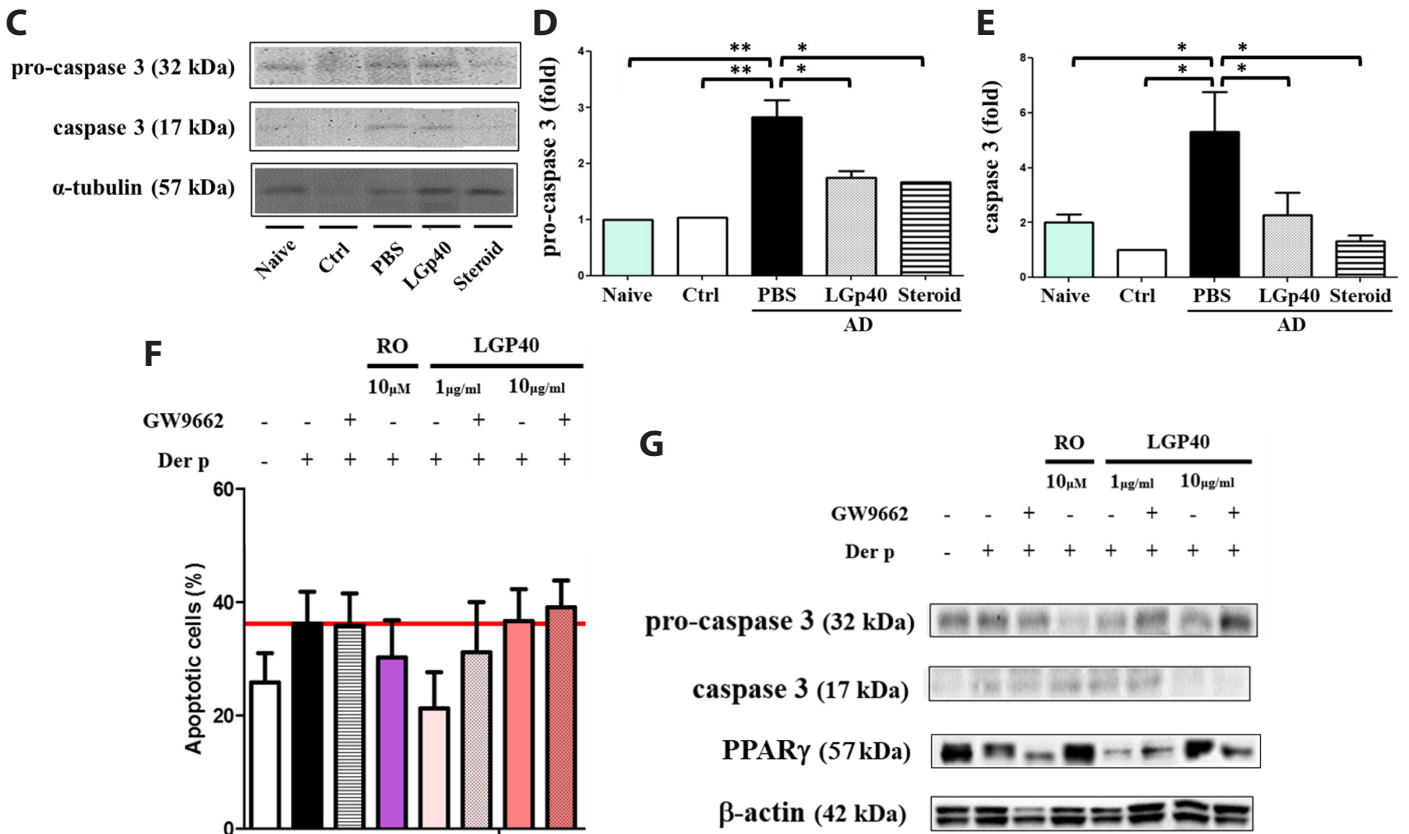
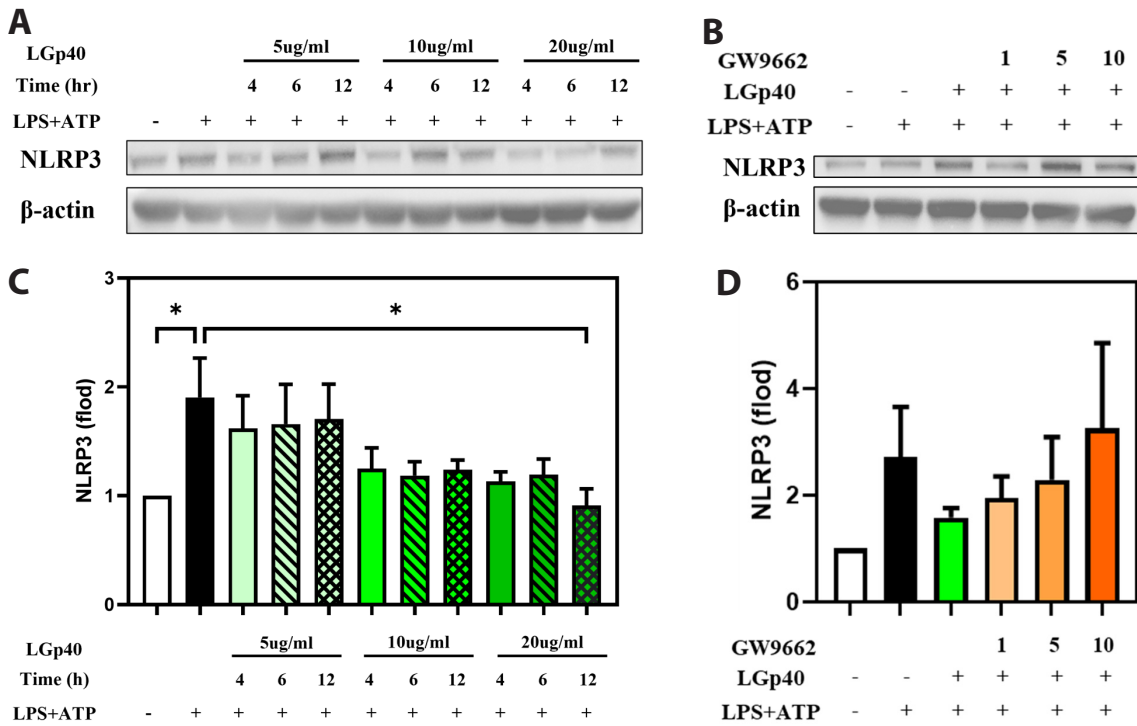


Figure 4. (Continued)



**Figure 5. LGp40 pretreatment suppressed NLRP3 expression and promoted PPAR $\gamma$  expression in the NLRP3 inflammasome cellular model.** THP-1 cells were incubated with LGp40 before LPS + ATP stimulation for NLRP3 inflammasome (n = 3). (A) Whole-cell extracts were analyzed by Western blotting with NLRP3 and  $\beta$ -actin antibodies. (B) Quantitative data of NLRP3. THP-1 cells were incubated with LGp40 and GW9662 (PPAR $\gamma$  antagonist) before LPS + ATP stimulation for NLRP3 inflammasome (n = 3). (C) Whole-cell extracts were analyzed by Western blotting with NLRP3 and  $\beta$ -actin antibodies. (D) Quantitative data of NLRP3. Protein expression levels were detected with densitometry and are depicted as proportional lines and bar graphs. The data represent the mean  $\pm$  SEM, \* $p$  < 0.05, \*\* $p$  < 0.01, Student's  $t$ -test.

### LGp40 inhibited the NLRP3 inflammasome

Activation of NLRP3 inflammasome was identified as an important trigger in the development of AD.<sup>12,13</sup> To explore the inhibitory function of LGp40 in NLRP3 inflammasome formation, an *in vitro* NLRP3 inflammasome activation model was developed in THP1 cells based on LPS priming and ATP activation. After LPS and ATP stimulation, THP1 cells had increased NLRP3 protein level. Pretreatment with LGp40 for 4 to 12 hours, and 5 to 20 µg/ml, induced a dose-dependent decrease in the protein level of NLRP3 (**Figure 5A, B**). To further explore whether the LGp40 inhibition of the NLRP3 inflammasome is PPAR $\gamma$  dependent, GW9662 was co-incubated in this cell culture system. The inhibitory effect of LGp40 on NLRP3 protein expression was reversed dose-dependently when GW9662 was co-incubated before NLRP3 inflammasome activation (**Figure 5C, D**). The data revealed that LGp40 also had an inhibitory effect on the NLRP3 inflammasome, and this effect may be PPAR $\gamma$  dependent.

### Discussion

The pathogenesis of AD is heterogeneous and involves an interplay of skin barrier disruption and immune-mediated inflammation. Both the “outside-in” and “inside-out” hypotheses likely hold true in different subsets of AD patients.<sup>14</sup> Most of the AD cases are initiated in infancy and persist into adulthood, whereas some AD cases develop for the first time in adulthood.<sup>1</sup> Food allergens are the most likely triggers in infants and young children with severe AD.<sup>1</sup> Adult-onset AD is associated with higher rates of sensitization to cross-reaction with food and airborne allergens, similar to that with house dust mite.<sup>1,15</sup> Therefore, we used both OVA and Der p allergens to trigger an AD-like mouse model in hairless SKH1 and hair-removed C57BL/6J strains based on the “outside-in” and “inside-out” hypotheses in this investigation. Both an OVA-induced “outside-in” SKH1 AD-like and a Der p-induced “inside-out” C57BL/6J AD-like mouse model were well-established (**Supplemental Figure 1-4**). The mice in these models displayed typical AD symptom of thick, shriveled epidermis. Furthermore, hallmarks of Th2 immunity were significant elevated in the lesion skin, but only SKH1 mice showed Th2/Th17-predominant AD endotype.

Probiotics decreased AD incidence by approximately 20%.<sup>16</sup> In this study, either *L. gasseri* or LGp40 supplementation in AD-like mice undertaken before and during allergens sensitization resolved the epidermal barrier dysfunction and immunologic abnormalities. The cutaneous lesion of AD-like mice healed to a fine, dewy skin state and the degrees of keratinocyte programmed cell death and local tissue inflammation decreased significantly. LGp40, a previously identified recombinant GAPDH protein,<sup>10</sup> is the main component of *L. gasseri* that activated the host PPAR $\gamma$  pathway in dendritic cells. Bacterial GAPDH is one of the moonlighting proteins that have glycolytic as well as extra-glycolytic functions, including host immunity modulation.<sup>17</sup> Although PPAR $\gamma$  activation in dendritic cells has controversial abilities in relation to airway allergic

inflammation,<sup>9,18,19</sup> PPAR $\gamma$  activation inhibited mucus and alarmin secretion in airway epithelial cells.<sup>20</sup> Our *in vitro* HaCaT keratinocytes model revealed that LGp40 upregulated PPAR $\gamma$  expression upon Der p exposure, but was unable to prevent cell apoptosis with a PPAR $\gamma$  antagonist. As PPAR $\gamma$  plays an important role in allergic disorders, we considered that *L. gasseri* may use the GAPDH protein to inhibit allergen-induced keratinocyte apoptosis via PPAR $\gamma$  activation. Nonetheless, the underlying mechanism of LGp40-induced PPAR $\gamma$ -dependent inhibition of cutaneous apoptosis needs future study.

Approximately 40% of AD patients present loss-of-function mutations in the *FLG* gene that damage the protective skin barrier against the external environment. This loose structure facilitates the penetration of *Staphylococcus aureus* and house dust mite to trigger skin inflammation.<sup>21,22</sup> *S. aureus* could activate the NLRP3 inflammasome in macrophages and mucosal membrane.<sup>23,24</sup> Mite allergen is a danger-regulator of NLRP3 inflammasome activation in keratinocytes and aggravated AD symptoms.<sup>12</sup> In a mouse model of chronic proliferative dermatitis, loss of *Nlrp3* attenuated skin inflammation and delayed disease onset,<sup>13</sup> suggesting that the NLRP3 inflammasome might be essential for disease development. Moreover, PPAR $\gamma$  agonists interfere with NLRP3 inflammasome formation and activation in macrophages or neurons.<sup>25,26</sup> Clinical thiazolidinedione drugs, which are synthetic ligands of PPAR $\gamma$ , attenuate caspase-1 maturation and decrease IL-1 $\beta$  and IL-18 production in NLRP3-associated diseases.<sup>27</sup> In this study, we have found that LGp40 might increase PPAR $\gamma$  expression to suppress the NLRP3 inflammasome, and the inhibitory effect was reversed with the PPAR $\gamma$  antagonist (**Figure 5**). Therefore, it is rational to infer that the NLRP3 inflammasome inhibition might mediate the protective effect of LGp40, which is also a type of PPAR $\gamma$ -dependent inhibition. Despite the controversial role of the NLRP3 inflammasome in the development of AD,<sup>27</sup> NLRP3 inhibition was associated with abrogated apoptosis in primary airway epithelial cells and induced resolution of allergic asthma.<sup>28</sup> Accordingly, our results suggest that LGp40 prevents skin inflammation and keratinocyte apoptosis through PPAR $\gamma$  activation and NLRP3 inflammasome inhibition and achieves an anti-allergy effect.

According to the guidelines for AD treatment, topical and systemic corticosteroids are appropriate therapeutic strategies in mild-to-moderate and severe AD, respectively.<sup>29</sup> Although steroids modulate allergen-induced strong Th2 immunity based on their significant anti-inflammatory and immunosuppressive effects, prolonged steroid application is usually accompanied by adverse effects. Long-term continual use of topical steroids may cause stinging sensation, dryness and thinning of the skin, leading to easy bruising and tearing of the skin.<sup>30</sup> In our Der p-induced AD mouse model, after using Dex, there was noticeable skin atrophy in the dorsal lesion skin which was evident as a thinning and translucency of the skin with telangiectasia. In contrast, these pathogenic phenomena were absent in the *L. gasseri* or the LGp40-treated groups.



Although the clinical applications of probiotic have been inconsistently reported from published clinical trials for decades,<sup>31</sup> probiotics as dietary supplements are generally considered safe and have been approved by regulatory authorities. The beneficial effect of probiotics in AD, based on recent investigative reports, may be attributable to multiple biological actions of the metabolites that are produced by probiotics. For example, D-tryptophan or short-chain fatty acids (SCFA), mainly butyrate, that are produced by *Lactobacillus* and *Bifidobacterium* can promote regulatory T-cell activation whereas they inhibit Th2 inflammation and lead to the suppression of allergic inflammation.<sup>32</sup> The SCFA-based mechanisms are largely mediated by the activation of certain G-protein-coupled receptors and/or the inhibition of histone deacetylases.<sup>33</sup> Microbial tryptophan metabolites, on the other hand, activate the aryl hydrocarbon receptor to modulate immune homeostasis.<sup>34</sup> Microbe-associated molecular patterns that are recognized by the toll-like receptor (TLR)2 and TLR4 play essential roles in restoring Th1/Th2 balance, and thereby regulate AD symptoms.<sup>35</sup> In this study, in addition to reprogramming macrophages,<sup>10</sup> we confirmed that GAPDH from *L. gasseri* mitigates cutaneous Th2 inflammation

and keratinocyte apoptosis through the activation of the PPAR $\gamma$  pathway. This result differs from other evidence that support the role of probiotic-regulated immune response in AD, which is mostly effected through microbial metabolites.

### Conclusions

In this study, a significant improvement of AD pathogenesis was observed in *L. gasseri*-supplemented mice and was accompanied by a decrease in Th2 and Th17 cells. Furthermore, direct application of LGp40 was effectively alleviated AD. The therapeutic potential of LGp40 is achieved by modulating cutaneous immune skewing, diminishing keratinocyte apoptosis via upregulation of PPAR $\gamma$ , and inhibiting the NLRP3 inflammasome (Figure 6). To our knowledge, this study is the first to confirm that *L. gasseri* may use moonlighting GAPDH proteins to alleviate both type 2 immunity and keratinocyte apoptosis in the AD lesion. This inhibitory effect might activate the PPAR $\gamma$  pathway to inhibit the NLRP3 inflammasome. The results of this study, when considered with previous research results, indicate a comprehensive mechanism for probiotics to prevent and treat allergic disorders, such as AD.

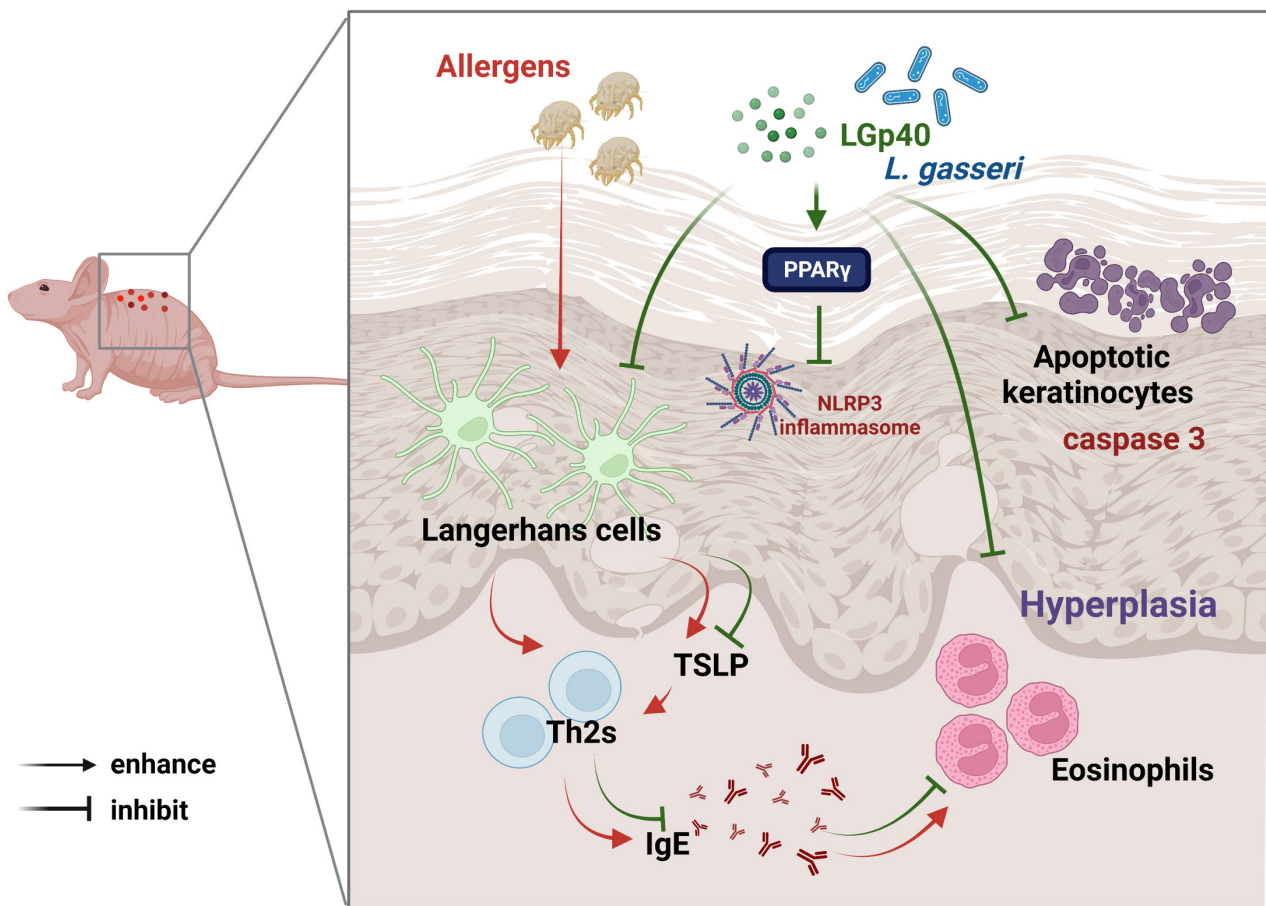


**Figure 6.** *L. gasseri* and its moonlighting LGp40 alleviated the cutaneous inflammatory responses in AD-like mice. The inhibitory effect involves the reduction of Langerhans cells infiltration and TSLP expression, with a resultant decline in Th2 inflammation. The reduction of the IgE level induces inhibition of eosinophilic infiltration of the AD lesion. Furthermore, LGp40 could inhibit keratinocyte apoptosis and the NLRP3 inflammasome through activation of the PPAR $\gamma$  pathway (The graph was created using BioRender.com).

## Acknowledgments

We thank Dr. Zi-Kai Lin (Department of Dermatological, Hualien Tzu Chi Hospital, Hualien, Taiwan) kindly provided SKH1 mice.

## Conflict of interests

The authors have declared that no competing interest exists.

## Funding

This work was funded through the following grants: NSTC 111-2113-M-039-003-MY2, MOST 110-2314-B-039-056 -MY3, and MOST 111-2113-M-039 -003 -MY2 from the National Science and Technology Council, Taiwan; the Headquarters of University Advancement at the National Cheng Kung University, sponsored by the Ministry of Education in Taiwan; a research grant (IJA8) from the Center for Allergy, Immunology, and Microbiome (A.I.M.), China Medical University Hospital, Taichung, Taiwan; ANHRF111-03 from the An Nan Hospital, China Medical University, Tainan, Taiwan; and DMR-112-205, DMR-112-043, and DMR-113-114 from the China Medical University Hospital, Taichung, Taiwan.

## Authors' contributions

- P.C.C, H.F.K, and J.Y.W conceived and designed the study.
- P.C.C purified the recombinant LGp40 proteins.
- M.H.H and Y.P.H performed the experiments of “outside in” mouse model.
- P.C.C and W.L.C performed the experiments of “inside out” mouse model.
- W.S.K and S.D.W performed the cell line experiments.
- W.S.K, L.S.H.W, S.D.W, and X.Y.L provided critical analysis and discussion.
- P.C.C, H.F.K, and J.Y.W wrote the manuscript.
- All authors approved the final manuscript for submission.

## References

- Weidinger S, Beck LA, Bieber T, Kabashima K, Irvine AD. Atopic dermatitis. *Nat Rev Dis Primers*. 2018;4(1):1.
- Sugaya M. The Role of Th17-Related Cytokines in Atopic Dermatitis. *Int J Mol Sci*. 2020;21(4).
- Leung DYM, Berdyshev E, Goleva E. Cutaneous barrier dysfunction in allergic diseases. *J Allergy Clin Immunol*. 2020;145(6):1485-97.
- Szymański U, Cios A, Ciepeliak M, Stankiewicz W. Cytokines and apoptosis in atopic dermatitis. *Postepy Dermatol Alergol*. 2021;38(2):1-13.
- Simon D, Lindberg RL, Kozłowski E, Braathen LR, Simon HU. Epidermal caspase-3 cleavage associated with interferon-gamma-expressing lymphocytes in acute atopic dermatitis lesions. *Exp. Dermatol*. 2006;15(6):441-6.
- Fang Z, Li L, Zhang H, Zhao J, Lu W, Chen W. Gut Microbiota, Probiotics, and Their Interactions in Prevention and Treatment of Atopic Dermatitis: A Review. *Front Immunol*. 2021;12:720393.
- Wang J, Wang JY. Children with atopic dermatitis show clinical improvement after Lactobacillus exposure. *Clin Exp Allergy*. 2015;45(4):779-87.
- Jan RL, Yeh KC, Hsieh MH, Lin YL, Kao HF, Li PH, et al. Lactobacillus gasseri suppresses Th17 pro-inflammatory response and attenuates allergen-induced airway inflammation in a mouse model of allergic asthma. *Br J Nutr*. 2012;108(1):130-9.
- Hsieh MH, Jan RL, Wu LS, Chen PC, Kao HF, Kuo WS, et al. Lactobacillus gasseri attenuates allergic airway inflammation through PPAR $\gamma$  activation in dendritic cells. *J Mol Med (Berl)*. 2018;96(1):39-51.
- Chen PC, Hsieh MH, Kuo WS, Wu LS, Kao HF, Liu LF, et al. Moonlighting glyceraldehyde-3-phosphate dehydrogenase (GAPDH) protein of Lactobacillus gasseri attenuates allergic asthma via immunometabolic change in macrophages. *J Biomed Sci*. 2022;29(1):75.
- Kopeckova M, Pavkova I, Stulik J. Diverse Localization and Protein Binding Abilities of Glyceraldehyde-3-Phosphate Dehydrogenase in Pathogenic Bacteria: The Key to its Multifunctionality? *Front Cell Infect Microbiol*. 2020;10:89.
- Dai X, Sayama K, Tohyama M, Shirakata Y, Hanakawa Y, Tokumaru S, et al. Mite allergen is a danger signal for the skin via activation of inflammasome in keratinocytes. *J Allergy Clin Immunol*. 2011;127(3):806-14.e1-4.
- Douglas T, Champagne C, Morizot A, Lapointe JM, Saleh M. The Inflammatory Caspases-1 and -11 Mediate the Pathogenesis of Dermatitis in Sharpin-Deficient Mice. *J Immunol*. 2015;195(5):2365-73.
- Silverberg NB, Silverberg JI. Inside out or outside in: does atopic dermatitis disrupt barrier function or does disruption of barrier function trigger atopic dermatitis? *Cutis*. 2015;96(6):359-61.
- Bumbacea RS, Corcea SL, Ali S, Dinica LC, Fanfaret IS, Boda D. Mite allergy and atopic dermatitis: Is there a clear link? (Review). *Exp Ther Med*. 2020;20(4):3554-60.
- Williams HC, Chalmers J. Prevention of Atopic Dermatitis. *Acta Derm Venereol*. 2020;100(12):adv00166.
- Sirover MA. Moonlighting glyceraldehyde-3-phosphate dehydrogenase: posttranslational modification, protein and nucleic acid interactions in normal cells and in human pathology. *Crit Rev Biochem Mol Biol*. 2020;55(4):354-71.
- Nobs SP, Natali S, Pohlmeier L, Okreglicka K, Schneider C, Kurrer M, et al. PPAR $\gamma$  in dendritic cells and T cells drives pathogenic type-2 effector responses in lung inflammation. *J Exp Med*. 2017;214(10):3015-35.
- Stark JM, Coquet JM, Tibbitt CA. The Role of PPAR- $\gamma$  in Allergic Disease. *Curr Allergy Asthma Rep*. 2021;21(11):45.
- Lakshmi SP, Reddy AT, Banno A, Reddy RC. Airway Epithelial Cell Peroxisome Proliferator-Activated Receptor  $\gamma$  Regulates Inflammation and Mucin Expression in Allergic Airway Disease. *J Immunol*. 2018;201(6):1775-83.
- Drislane C, Irvine AD. The role of filaggrin in atopic dermatitis and allergic disease. *Ann Allergy Asthma Immunol*. 2020;124(1):36-43.
- Seiti Yamada Yoshikawa F, Feitosa de Lima J, Notomi Sato M, Álefe Leuzzi Ramos Y, Aoki V, Leao Orfali R. Exploring the Role of Staphylococcus Aureus Toxins in Atopic Dermatitis. *Toxins*. 2019;11(6).
- Craven RR, Gao X, Allen IC, Gris D, Bubeck Wardenburg J, McElvania-Tekippe E, et al. Staphylococcus aureus alpha-hemolysin activates the NLRP3-inflammasome in human and mouse monocytic cells. *PLoS One*. 2009;4(10):e7446.
- McGilligan VE, Gregory-Ksander MS, Li D, Moore JE, Hodges RR, Gilmore MS, et al. Staphylococcus aureus activates the NLRP3 inflammasome in human and rat conjunctival goblet cells. *PLoS One*. 2013;8(9):e74010.
- Yang CC, Wu CH, Lin TC, Cheng YN, Chang CS, Lee KT, et al. Inhibitory effect of PPAR $\gamma$  on NLRP3 inflammasome activation. *Theranostics*. 2021;11(5):2424-41.
- Meng QQ, Feng ZC, Zhang XL, Hu LQ, Wang M, Zhang HF, et al. PPAR- $\gamma$  Activation Exerts an Anti-inflammatory Effect by Suppressing the NLRP3 Inflammasome in Spinal Cord-Derived Neurons. *Mediators Inflamm*. 2019;2019:6386729.
- Tang L, Zhou F. Inflammasomes in Common Immune-Related Skin Diseases. *Front Immunol*. 2020;11:882.
- Lv J, Su W, Yu Q, Zhang M, Di C, Lin X, et al. Heme oxygenase-1 protects airway epithelium against apoptosis by targeting the proinflammatory NLRP3-RXR axis in asthma. *J Biol Chem*. 2018;293(48):18454-65.
- Eichenfield LF, Tom WL, Berger TG, Krol A, Paller AS, Schwarzenberger K, et al. Guidelines of care for the management of atopic dermatitis: section 2. Management and treatment of atopic dermatitis with topical therapies. *J Am Acad Dermatol*. 2014;71(1):116-32.

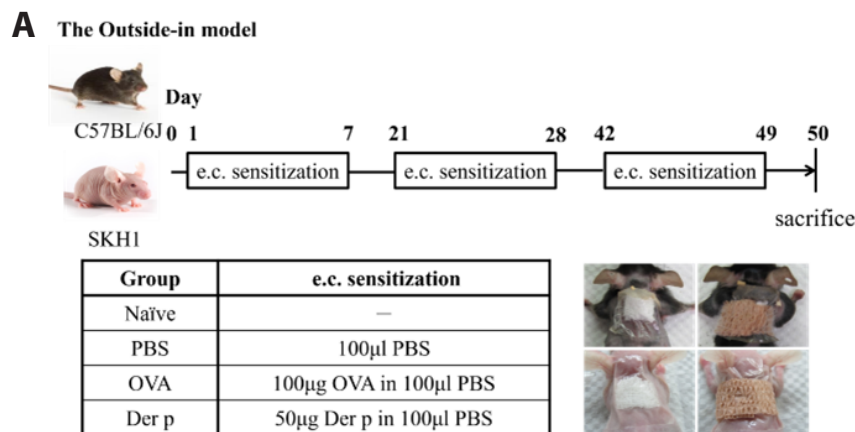
30. Stacey SK, McEleney M. Topical Corticosteroids: Choice and Application. *Am Fam Physician*. 2021;103(6):337-43.
31. Doron S, Snyderman DR. Risk and safety of probiotics. *Clin Infect Dis*. 2015;60 Suppl 2(Suppl 2):S129-34.
32. Schwarz A, Bruhs A, Schwarz T. The Short-Chain Fatty Acid Sodium Butyrate Functions as a Regulator of the Skin Immune System. *J Invest Dermatol*. 2017;137(4):855-64.
33. Alam MJ, Xie L, Yap YA, Marques FZ, Robert R. Manipulating Microbiota to Treat Atopic Dermatitis: Functions and Therapies. *Pathogens*. 2022;11(6).
34. Zelante T, Iannitti RG, Cunha C, De Luca A, Giovannini G, Pieraccini G, et al. Tryptophan catabolites from microbiota engage aryl hydrocarbon receptor and balance mucosal reactivity via interleukin-22. *Immunity*. 2013;39(2):372-85.
35. Zhang Y, Wang HC, Feng C, Yan M. Analysis of the Association of Polymorphisms rs5743708 in TLR2 and rs4986790 in TLR4 with Atopic Dermatitis Risk. *Immunol Invest*. 2019;48(2):169-80.

## Supplemental file

### The “outside-in” mouse models of AD

In this study, the protection effect of *L. gasseri* and its moonlighting recombinant GAPDH (LGp40) were investigated in the “outside-in” and “inside-out” mouse models of AD. To establish the “outside-in” AD mouse model, both C57BL/6J and SKH1 (hairless) mice were percutaneously sensitized with either OVA or Der p over 7 weeks (Supplementary Figure S1A). Application of both OVA and Der p allergens on the dorsal skin of C57BL/6J mice induced a steady increase in sera concentrations of total IgE, OVA-specific IgE, and Der p-specific IgE. In SKH1 mice, only OVA percutaneous sensitization induced an increase in the total IgE level and the allergen-specific IgE concentrations (Supplementary Figure S1B, C). OVA or Der p allergen stimulation induced the characteristic dry and scaly skin of AD in SKH1 mice along with increased trans-epidermal water loss (TEWL) as compared with the Naïve and PBS controls (Supplementary Figure S1D, E).

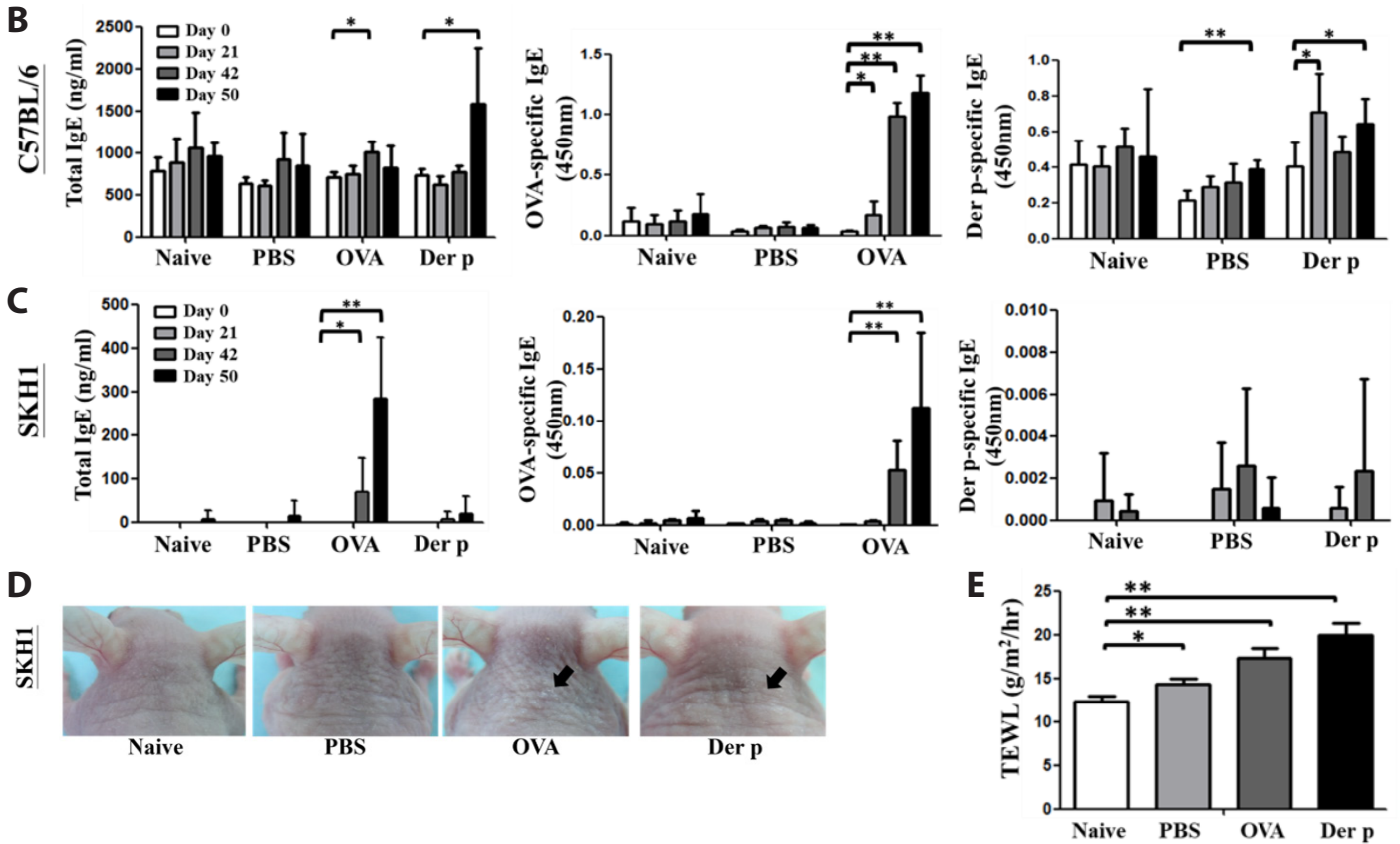
Increases in epidermal and dermal thickness were also observed in OVA or Der p -induced C57BL/6J and SKH1 AD-like mice, particularly in OVA-induced SKH1 AD-like mice in comparison with controls ( $p < 0.01$ ) (Supplementary Figure S2A, B). Furthermore, SKH1 AD-like mice showed significantly increased of eosinophil and Langerhans cell infiltrations in skin lesions in both allergen-induced groups. In Naïve and PBS groups, most of the Langerhans cells were present in the epidermis whereas, in allergen-sensitized groups, the activated Langerhans cells were found mostly in the dermis rather than in the epidermis in the lesion (Supplementary Figure S2C-E). Furthermore, the TSLP and RORyt expression in skin lesions in both allergen-induced AD-like SKH1 mice enhanced (Supplementary Figure S2F, G). These findings revealed that OVA-sensitized SKH1 AD-like mice was compatible with an “outside-in” AD mouse model, and were used in the following studies.



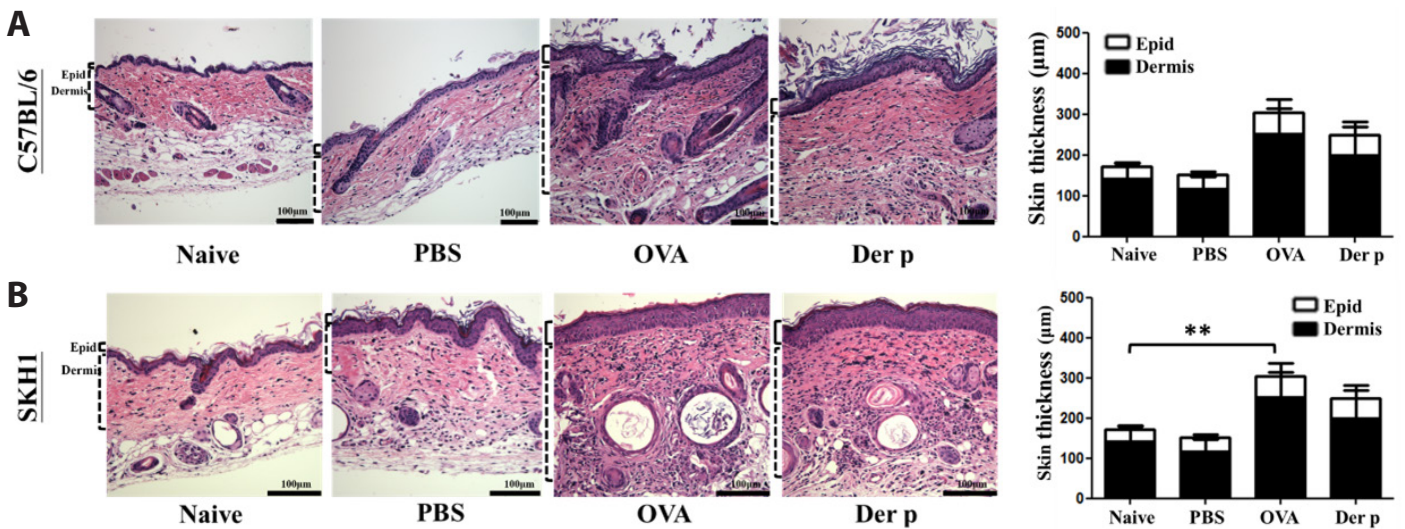
### Supplementary Figure S1. The characteristics of sera IgE and cutaneous physiology of the “outside-in” AD model.

(A) “Outside-in” mouse model of AD. C57BL/6J and SKH1 mice were divided into four groups (Naïve, PBS, OVA and Der p) and were epicutaneously (e.c.) sensitized to allergens (animal experimental model protocol 1). (B) Total IgE, OVA-specific IgE, and Der p-specific IgE levels in sera of C57BL/6J mice model (n = 4 mice). (C) Total IgE, OVA-specific IgE, and Der p-specific IgE levels in sera of SKH1 mice model (n = 3 mice). The IgE levels were measured using ELISA. (D) Morphology of lesional skin in SKH1 mice model (n = 3 mice). (E) TEWL values of skin were measured by Tewameter TM210 (n = 3 mice). The data represent the mean ± SEM, \* $p < 0.05$ , \*\* $p < 0.01$ , Student’s *t*-test.



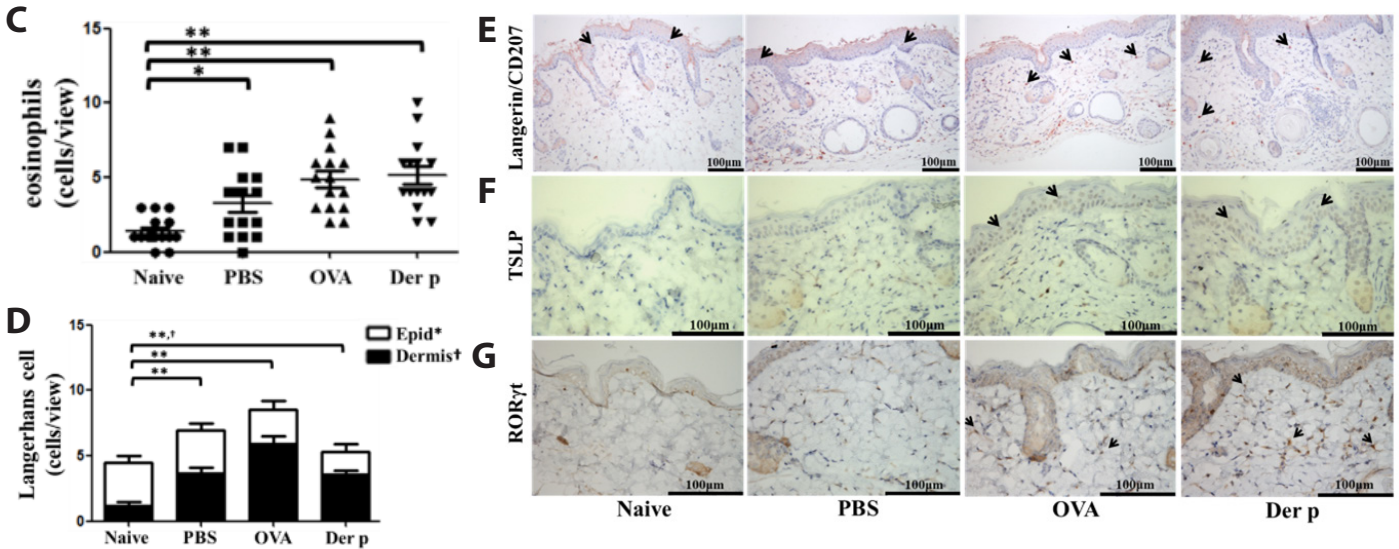


Supplementary Figure S1. (Continued)



Supplementary Figure S2. The characteristics of cutaneous pathology and immunology of the “outside-in” AD model.

Lesional skin histology and measurement of the epidermal and dermal thickness in (A) C57BL/6J mice model (n = 4 mice) and in (B) SKH1 mice model (n = 3 mice). Skin sections were stained with H&E. (C) Infiltrated eosinophils in the cutaneous tissue of SKH1 mice were counted. The data represent the mean ± SEM (n = 3 mice), \**p* < 0.05, \*\**p* < 0.01, Student's *t*-test. (D) Infiltrated Langerhans cells (black arrows at section in the cutaneous tissue of SKH1 mice model were counted. The data represent the mean ± SEM (n = 3 mice), \*\**p* < 0.01 of epidermis, \**p* < 0.05 of dermis, Student's *t*-test. Skin sections of SKH1 mice model were immunostained with (E) langerin/CD207, (F) TSLP, and (G) RORγt antibodies and reacted with AEC or DAB. The data represent the mean ± SD, \**p* < 0.05, \*\**p* < 0.01, Student's *t*-test.

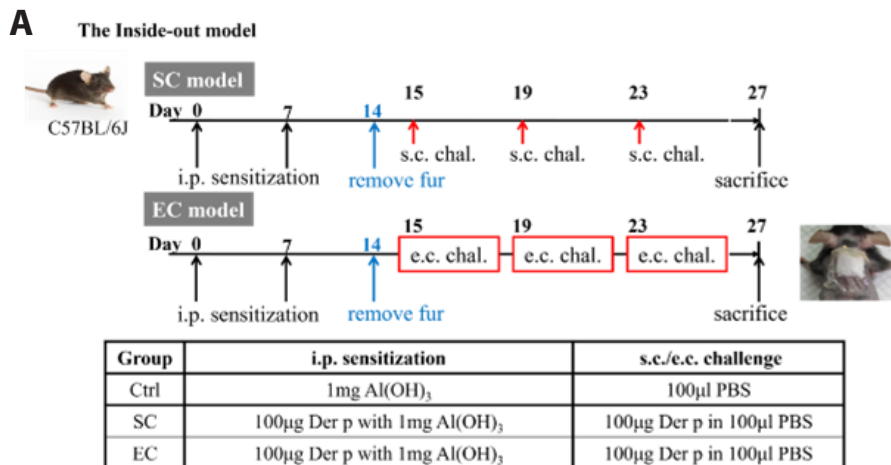


Supplementary Figure S2. (Continued)

**The “inside-out” mouse model of AD**

The “inside-out” AD mouse model was also established in C57BL/6J and SKH1 mice (Supplementary Figure S3A, B). The mice were intraperitoneally sensitized and then percutaneously challenged with Der p allergen as specified in the protocol. Der p-sensitized C57BL/6J and SKH1 AD-like mice exhibited a sustained elevation of total IgE and Der p-specific IgE (Supplementary Figure S3C, D). A wrinkled skinfold with rough, scaly patches and dehydrated skin were observed in these AD-like mice. Furthermore, both SC and EC groups of C57BL/6J AD-like mice showed delayed hair growth and prolonged hair loss as compared with Ctrl group (Supplementary Figure S3E, F). Der p-sensitized SKH1 AD-like mice had significantly

enhanced TEWL as compared with Naïve group (Supplementary Figure S3G). In further studies in the AD skin lesion of C57BL/6J AD-like mice, we noted enhancement of dermal thickness, increased infiltration by eosinophils and Langerhans cells, and TSLP expression (Supplementary Figure S4A-E). In contrast, there was no significant change in the dermal thickness or increased eosinophil and Langerhans cell infiltration, or enhanced TSLP expression in the AD skin lesions of SKH1 AD-like mice (Supplementary Figure S4F-J). These findings indicated that the Der p-sensitized and challenged C57BL/6J mice were more compatible than the SKH1 mice for the “inside-out” AD mouse model, and were used in the following studies.



Supplementary Figure S3. The characteristics of sera IgE and cutaneous physiology of the “inside-out” AD model.

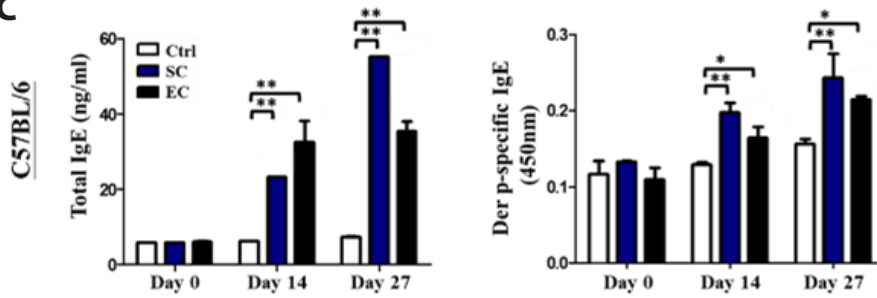
“Inside-out” mouse model of AD in (A) C57BL/6J and (B) SKH1 mice. C57BL/6J mice were divided into three groups. Ctrl group was intraperitoneally (i.p.) sensitized with PBS. The other groups were i.p. sensitized with Der p to induce AD through subcutaneous (s.c.) challenge (SC group) or epicutaneous (e.c.) challenge (EC group) (animal experimental model protocol 2). SKH1 mice were divided into two groups. They were both i.p. sensitized with Der p. D-PBS and Der p group were e.c. challenged by skin coverage with a 1×1 cm square of sterile gauze that contained either PBS or 50 µg Der p for 14 consecutive days. Total IgE and Der p-specific IgE levels in sera of (C) C57BL/6J mice model and (D) SKH1 mice model. The IgE levels were measured using ELISA. Morphology of lesional skin in (E) C57BL/6J and (F) SKH1 mice model. (G) TEWL values of SKH1 mice skin were measured by Tewameter TM210. The data represent the mean ± SEM (n = 6 mice), \*p < 0.05, \*\*p < 0.01, Student’s t-test.

**B The Inside-out model**

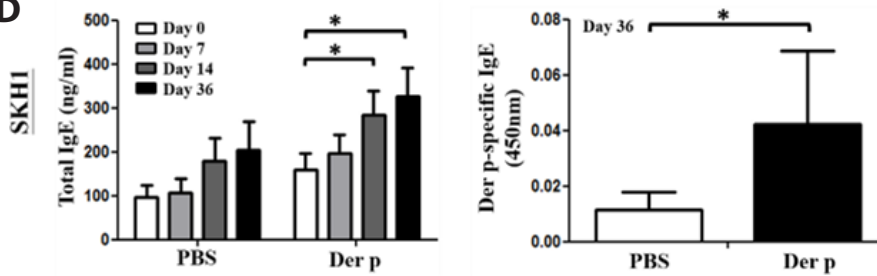


Group	i.p. sensitization	e.c. challenge
D-PBS	50µg Der p with 1mg Al(OH) <sub>3</sub>	100µl PBS
Der p	50µg Der p with 1mg Al(OH) <sub>3</sub>	50µg Der p in 100µl PBS

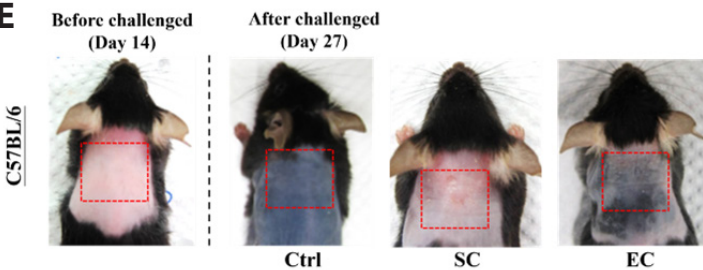
**C**



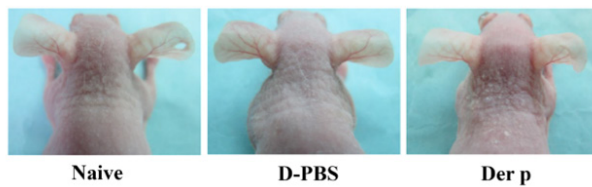
**D**



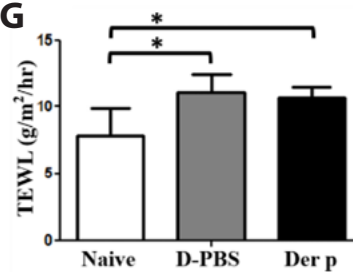
**E**



**F**

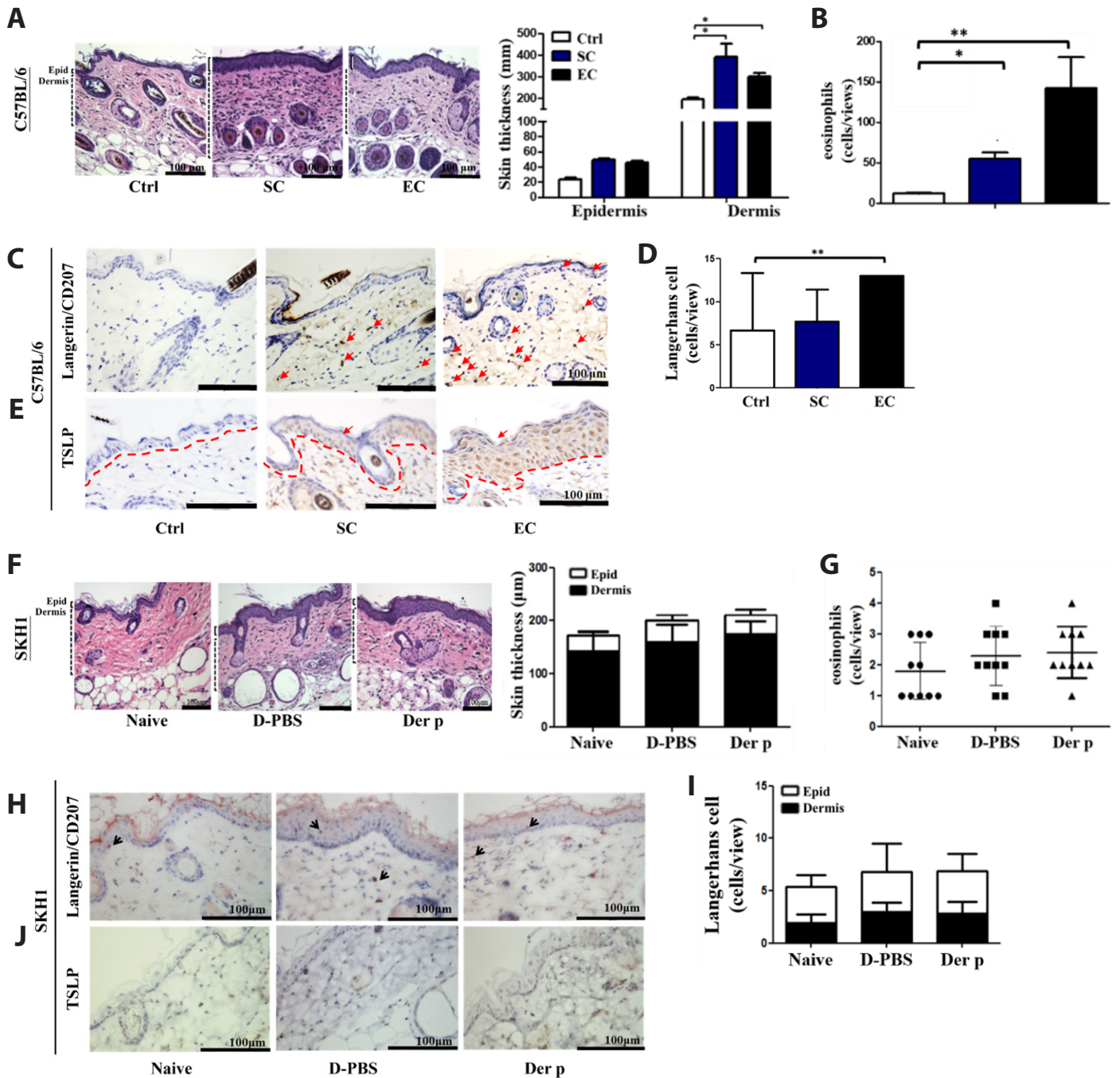


**G**



Supplementary Figure S3. (Continued)





**Supplementary Figure S4. The characteristics of cutaneous pathology and immunology of the “inside-out” AD model.**

(A) Lesional skin histology, measurement of epidermis and dermis thickness, and (B) numbers of infiltrated eosinophils in the cutaneous tissue of C57BL/6J mice model. Skin sections of C57BL/6J mice model were immunostained with (C) langerin/CD207 antibody and (D) the positive cell (red arrows) in the cutaneous tissue were counted. Skin sections of C57BL/6J mice model were also immunostained with (E) TSLP antibodies and reacted with DAB. (F) Lesional skin histology, measurement of epidermis and dermis thickness, and (G) numbers of infiltrated eosinophils in the cutaneous tissue of SKH1 mice model. Skin sections of SKH1 mice model were immunostained with (H) langerin/CD207 antibody and (I) the positive cell (red arrows) in the cutaneous tissue were counted. Skin sections of SKH1 mice model were also immunostained with (J) TSLP antibodies and reacted with DAB. The data represent the mean ± SEM (n = 6 mice), \**p* < 0.05, \*\**p* < 0.01, Student’s t-test.